ORIGINAL PAPER

INVESTIGATION OF CYTOTOXICITY AND ANTIBACTERIAL EFFECT OF BORON-CONTAINING NANO-HYDROXYAPATITE

Numan Aydın[1], Serpil Karaoğlanoğlu[1], Aysun Kılıç Süloğlu[2], Neslihan İdil[2], Merve Demir[2], İbrahim Hakkı Karakaş[3]

[1]Department of Restorative Dental Treatment, University of Health Sciences, Gulhane Faculty of Dentistry, Ankara, Turkey
[2]Department of Biology, Faculty of Science, Hacettepe University, Ankara, Turkey
[3]Engineering Faculty, Bayburt University, Bayburt, Turkey

ABSTRACT

Introduction: Different regenerative materials are used to protect and stimulate pulp tissue.

Objectives: This *in vitro* study aimed to examine the cytotoxicity of different doses of boron-containing nano-hydroxyapatite (B-nHAp) and its antibacterial effect.

Material and methods: B-nHAp was synthesized with microwave-assisted chemical precipitation method at different rates, such as 1%, 5%, and 10%. The extracts were prepared in separate tubes: 1%, 5%, 10% B-nHAp, and nHAp 50 mg/ml. Cytotoxicity test was performed on L929 mouse fibroblasts for 24 and 72 hours. Antibacterial analysis was performed with *Streptococcus mutans* bacteria using micro-dilution method. Cell viability values were evaluated with two-way analysis of variance (ANOVA) test ($p < 0.05$).

Results: B-nHAp was successfully synthesized in XRD and SEM analyses. Nano-hydroxyapatite showed more cell viability than control group at 24 and 72 hours. All B-nHAp extracts demonstrated less cell viability at the end of 24 hrs. than control group. However, 1% B-nHAp cell viability decreased more in the B-nHAp group compared with the control group, while 5% and 10% B-nHAp showed high cell viability after 72 hours of incubation. B-nHAp demonstrated less antibacterial effect on *Streptococcus mutans* compared with nHAp.

Conclusions: According to the results, the addition of boron to nano-hydroxyapatite does not make a significant contribution to increase the regenerative and antibacterial properties of the material.

Key words: nano-hydroxyapatite, boron, cytotoxicity, *Streptococcus mutans*.

J Stoma 2024; 77, 2: 93-99
DOI: https://doi.org/10.5114/jos.2024.139890

INTRODUCTION

Dental pulp, the only soft connective tissue between mineralized tissues in the structure of tooth, is vulnerable to infections caused by different irritants, showing limited regenerative capacity [1, 2]. The viability of pulp depends on its structural components, which are vascularized and innervated [3]. Pulp stem cells constitute an important part of pulp cells, and are usually located in the perivascular area, where nerve endings are abundant [4]. They have strong potential for neuro-genesis, angio-genesis, and neuro-vascular inductive activity [5]. Pulp stem cells renew odontoblasts upon stimulation during dentin repair [5, 6].

Stem cell-based therapies and dental tissue engineering are new strategies to stimulate both the structural and physiological roles of the tooth [7]. Bioactive glasses easily react with physiological fluids and form a stable interface with hard tissue through the formation of a hydroxyapatite (HA) layer [8]. Boron-doped

JOURNAL OF STOMATOLOGY
CZASOPISMO STOMATOLOGICZNE

Address for correspondence: Numan Aydın, DDS, PhD, Department of Restorative Dental Treatment, Gulhane Faculty of Dentistry, University of Health Sciences, Etlik 06018, Ankara, Turkey, phone: +90-3123043000, e-mail: dt_numan@hotmail.com

Received: 10.10.2022 • Accepted: 05.10.2023 • Published: 29.05.2024

bioactive glasses have been used in tissue engineering scaffolds due to their biological properties, such as increased release of cytokines and increased extra-cellular matrix cycle [9]. Studies have reported that boron increase the osteogenic and odontogenic differentiation of human tooth germ stem cells (hTGSCs) [10]. High doses of boric acid reduce the viability of dental pulp stem cells (DPSCs) [11], mouse osteoblasts [12], human bone marrow mesenchymal stem cells (hBMSCs) [13], and rat bone marrow mesenchymal stem cells (rBMSCs) [14]. The antibacterial effect of boric acid that is generally used as an antiseptic agent in medical field, has been recognized in dentistry. As a result of systemic administration of boric acid, periodontal inflammation and alveolar bone loss decrease [15]. Boric acid is not toxic to periodontal ligament stem cells at concentrations of 0.5% and 0.75%, and does not inhibit their proliferation, migration, or adhesion to root surfaces [16].

Hydroxyapatite is a bioactive, biocompatible, glass-like bio-ceramic that replaces the inorganic extra-cellular matrix of enamel and dentin. nHAp can be used in the regeneration of bone cells, dentin hypersensitivity, and prevention of dental caries [17]. In caries prevention, it has also been incorporated into toothpastes to provide ions that reduce de-mineralization and improve re-mineralization [18].

In this study, B-nHAp was synthesized by a chemical precipitation method to combine the positive properties of these two materials. Then, cytotoxicity of the synthesized different B-nHAp doses on L929 mouse fibroblasts and antibacterial effect on *Streptococcus mutans* ATCC 25175 were investigated *in vitro*.

MATERIAL AND METHODS

SYNTHESIS OF BORON-CONTAINING NANO-HYDROXYAPATITE

In this study, B-nHAp nano-particles containing boron at three different rates, i.e., 1%, 5%, and 10%, were synthesized via microwave-assisted chemical precipitation method. All chemicals used in the study were purchased from Sigma-Aldrich (USA), and no additional purification was applied [19]. According to this method, a certain amount of calcium nitrate ($Ca(NO_3)_2\ 4H_2O$) was dissolved in double distilled water. Then, ammonium hydrogen phosphate ($(NH_4)_2\ HPO_4$) was added to the calcium nitrate solution. Quantities of these reagents were determined according to the reaction provided with Equation 1:

$$30\ Ca(NO_3)_{2(aq)} + 18\ (NH_4)_2HPO_{4(aq)} + 64\ NH_3$$
$$3\ Ca10\ (PO_4)_6(OH)_{2(k)} + 80\ N_{2(g)} + 174\ H_2O\ (s)$$

Next, boric acid (H_3BO_3) was added to the mixture in a pre-determined amount, and pH value of the mixture was adjusted to 10 using concentrated ammonia solution (NH_4OH). After the mixture was effectively stirred using a magnetic stirrer (Heidolph, Germany) for about 30 minutes, the final solution was placed in a kitchen-type microwave oven (Arçelik, Turkey), and it was subjected to microwave radiation (800 W) for about 15 minutes. At the end of the process, the mixture was filtered by a vacuum filtration system, and the obtained solid sample was dried at 150°C during 12 hrs. in a drying oven. The final sample was subjected to heat treatment for 2 hrs. at 1,000 in a muffle furnace (Carbolite, UK). The sample taken from the furnace was placed into a desiccator to protect from ambient moisture. Flow chart for the applied synthesis process is presented in Figure 1.

XRD (X-ray diffraction) analysis was performed to determine the structural properties of the prepared samples, and SEM analysis was performed to examine the micro-structure properties. XRD analyses of the synthesized material were done with a Bruker D8 Discover X-Ray diffractometer, and SEM analyses were performed with a FEI NNS450-FEG SEM system.

PREPARATION OF EXTRACTS

The extracts were prepared in separate tubes as 50 mg/ml B-nHAp and nHAp, synthesized at 1%, 5%, and 10%. After being incubated at 37°C for 24 hours, the prepared extracts were diluted with serum-free growth culture Dulbecco's modified eagle's medium (DMEM; Cegrogen Biotech GmbH, Stadtallendorf, Germany) at a rate of 1 : 2, 1 : 4, 1 : 8, and 1 : 16 before being used in cell culture analysis. L929 cells were used as the control group.

CELL CULTURE

The L929 fibroblast cell line used in the study was removed from storage at –196°C and dissolved in a water bath at 37°C. The cells were routinely retained in 10% fetal bovine serum (PAA Laboratories, Linz, Austria) and 1% antibiotic (100 U penicillin/100 µg streptomycin antibiotic; Capricorn Scientific, Germany) containing DMEM at 37°C and with 5% CO_2 incubator. Once the cells reached confluency, the cell suspension was prepared as described in ISO 10993-5:2009 (1×10^5 cells/ml) by calculating the cell number of the desired density for a 96-well cell culture plate using DMEM. This cell suspension was incubated for 24 hrs. in a 96-well cell culture plates (100 µL/well). After incubation for 24 hours, DMEM was removed, and the medium of five different dilutions, in which the filling materials were kept was placed in the wells (100 µl/well) and incubated for 24 and 72 hours. Then, MTT test was performed.

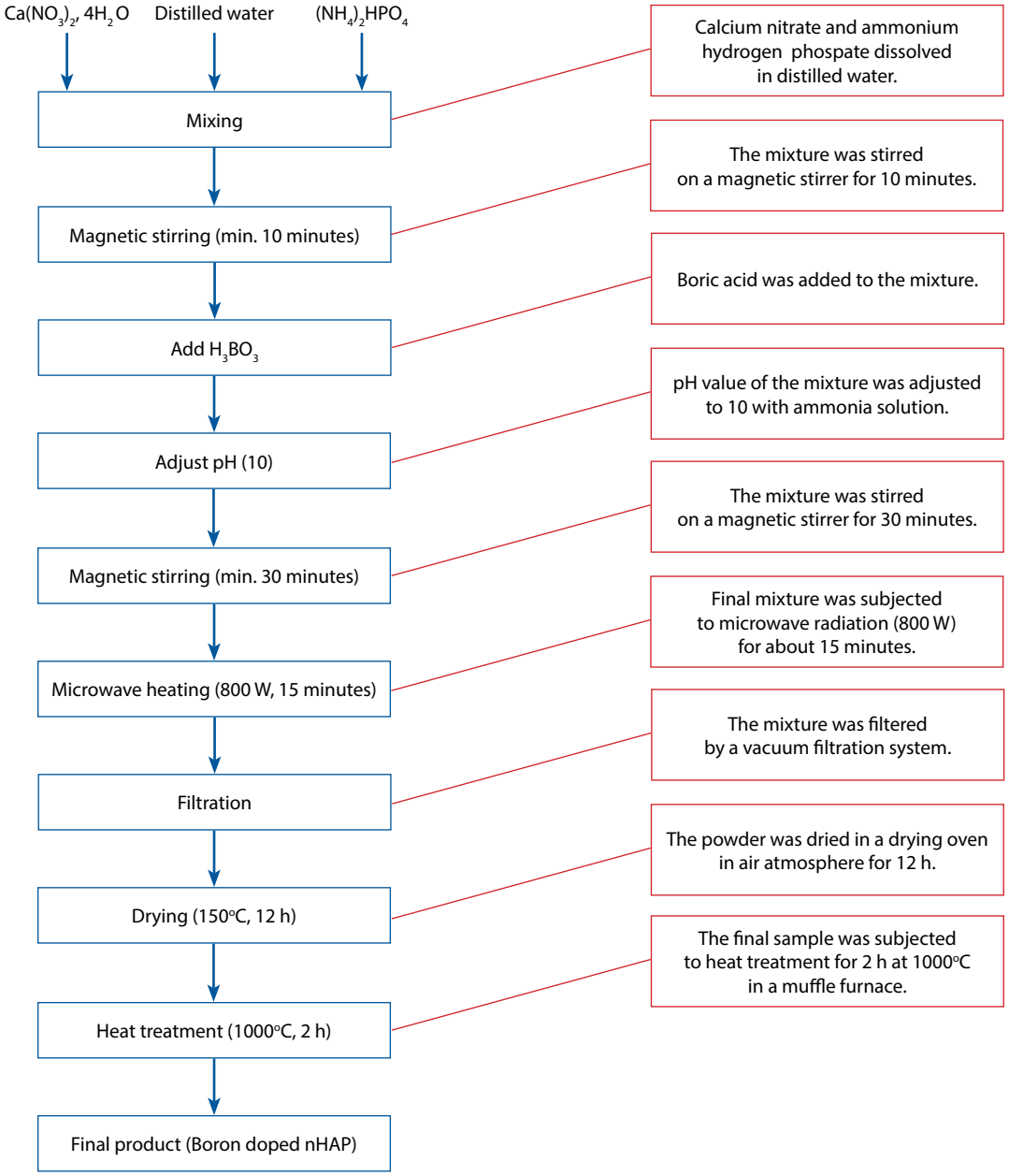

FIGURE 1. Flow chart of the applied synthesis process

CYTOTOXICITY TEST

MTT (3-(4.5-dimethylthiazol-2-il)-2.5-diphenyltetrazolium bromide); Sigma, USA) was mixed with phosphate-buffered saline (PBS) (Thermo Fisher, 003002), homogenized, and the MTT solution with a final concentration of 5 mg/ml was prepared. The medium of the cells incubated in the 96-well cell culture plate for 24 hours was aspirated. Then, 13 µl/well MTT solutions were applied to the cells and incubated for 4 hours in a dark environment at 37°C. After incubation, the MTT solution was removed and 100 µl/well dimethyl sulfoksit (DMSO) (Applichem, 01A3672, 0100), Ammonia; Merck K13391922) Ammonia-DMSO 5:100) mixture was added to dissolve formazan crystals. The absorbance was measured at 550 nm using a microplate reader (BIO-TEK uQuant, BIO-TEK Instruments, Inc., USA). The experiments were carried out in triplicate, and the percentage of viable cells was defined as the treatment and control groups (the control group was assumed to be 100% survival).

ANTIBACTERIAL ANALYSIS

Antibacterial activities of B-nHAp synthesized at different rates (1%, 5%, and 10%) were determined by the modified micro-dilution method. First, *Streptococcus mutans* ATCC 25175 was inoculated into a brain heart infusion (BHI) fluid medium (50 ml) and incubated at 37°C for 18 hours. Turbidity of the bacterial cell suspen-

sion was measured at 620 nm with a spectrophotometer, and adjusted according to a 0.5 McFarland standard (1–1.5 × 10^8 cfu/ml). Of this bacterial suspension, 200 µl was inoculated into BHI medium containing 1 : 1, 1 : 2, 1 : 4, 1 : 8, and 1 : 16 diluted B-nHAp and nHAp solutions. Following the incubation step of 24 hours at 37°C, turbidity measurement was performed with a spectrophotometer at 620 nm. To determine the initial bacterial turbidity, 200 µl *Streptococcus mutans* was inoculated into B-nHAp and nHAp-free medium and incubated under the same conditions. After measuring absorbance values of the first and last bacterial suspensions in the samples, relative bacterial inhibition growth (%) was calculated according to the formula given below:

Relative bacterial inhibition growth (%): ((Ai – Af)/Ai) × 100,

where *Ai* is an average of six replicates of absorbance at 620 nm of the initial bacterial suspensions, and *Af* is an average of six replicates of absorbance at 620 nm of the final bacterial suspensions.

STATISTICAL ANALYSIS

Statistical analysis of data was performed using SPSS 22.0 (SPSS Inc., Chicago, IL, USA). Cell viability values of nHAp and B-nHAp at the end of 24 and 72 hours were evaluated using two-way analysis of variance (ANOVA) and Tukey's multiple comparison test ($p < 0.05$). Antibacterial effects of nHAp and B-nHAp (1%, 5%, and 10%) on *Streptococcus mutans* were evaluated using two-way analysis of variance (ANOVA) and Tukey's multiple comparison test ($p < 0.05$).

RESULTS

XRD AND SEM ANALYSES

X-ray diffractograms of the samples containing 1%, 5%, and 10% boron of nano-hydroxyapatite are presented in Figure 2, and SEM images are shown in Figure 3. In the comparison of X-ray diffractograms with standard databases, the X-ray patterns obtained were fully compatible with the standard diffraction card (ICDD-PDF 00-001-1008) that was defined for hydroxyapatite, and all reflection peaks defined for this structure on this card were obtained. Furthermore, no peak resulting from the added H_3BO_3 was recorded. Accordingly, the added H_3BO_3 degraded into an amorphous structure in the reaction, and did not change the crystal structure.

The synthesized samples in SEM images consisted of nano-scale particles with a relatively homogeneous shape size distribution. The particles obtained in all three samples containing different amounts of boron were very close to each other in terms of morphological properties. In addition, the increase in the amount

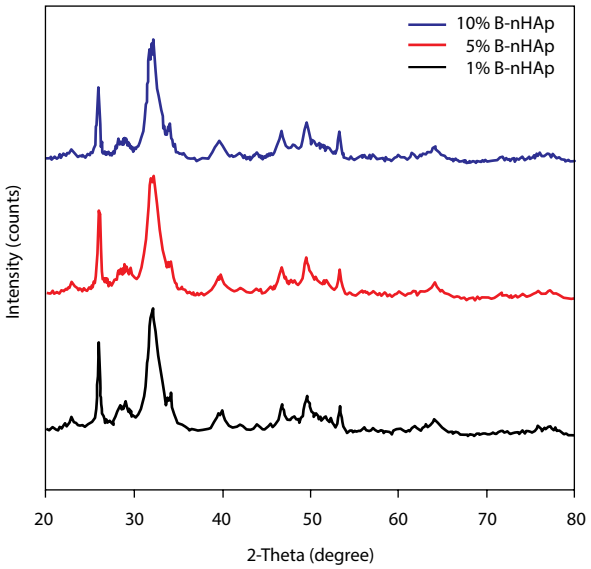

FIGURE 2. X-ray diffractograms of boron-containing nano-hydroxyapatite. Black: 1% B-nHAp, red: 5% B-nHAp, blue: 10% B-nHAp

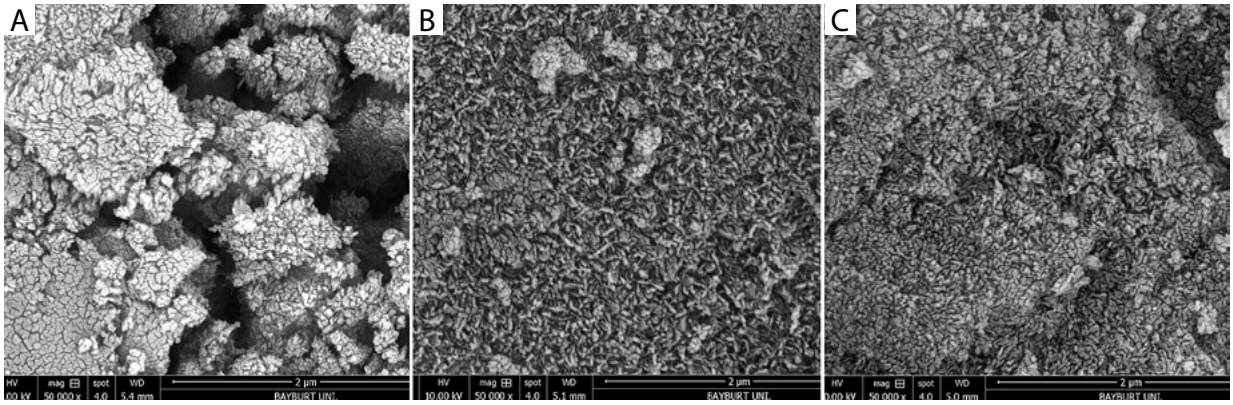

FIGURE 3. SEM images of boron-containing nano-hydroxyapatite. A) 1% B-nHAp, B) 5% B-nHAp, C) 10% B-nHAp

TABLE 1. Cell viability percentages of the extracts of nHAp and B-nHAp (1%, 5%, and 10%) in different dilutions at the end of 24 hours

Material/dilution ratio	nHAp	1% B-nHAp	5% B-nHAp	10% B-nHAp
1 : 1	$10.1 \pm 1.5^{a,A}$	$47.9 \pm 5.7^{a,B}$	$7.3 \pm 0.3^{a,A}$	$7.4 \pm 0.5^{a,A}$
1 : 2	$118.7 \pm 9.4^{b,A}$	$79.6 \pm 4.9^{b,B}$	$76.6 \pm 2.4^{b,B}$	$64.6 \pm 6.7^{b,C}$
1 : 4	$108.3 \pm 5.3^{c,A}$	$88.8 \pm 5.2^{c,B}$	$73.4 \pm 3.2^{b,C}$	$80.5 \pm 8.7^{c,BC}$
1 : 8	$94.3 \pm 3.6^{d,A}$	$90.9 \pm 4.2^{c,A}$	$76.4 \pm 1.5^{b,B}$	$80.2 \pm 3.7^{c,B}$
1 : 16	$99.5 \pm 3.5^{d,A}$	$84.4 \pm 3.9^{bc,B}$	$84.9 \pm 7.4^{c,B}$	$88.7 \pm 9.6^{c,B}$
Control (DMEM)	100.0 ± 5.2^{d}	100.0 ± 5.2^{d}	100.0 ± 5.2^{d}	100.0 ± 5.2^{d}

**Statistical difference between concentration rates of materials is shown as 'a-d', and statistical difference between nHAp and B-nHAp (1%, 5%, and 10%) is shown as 'A-C'; $p < 0.001$*

TABLE 2. Cell viability percentages of the extracts of nHAp and B-nHAp (1%, 5%, and 10%) in different dilutions at the end of 72 hours

Material/dilution ratio	nHAp	1% B-nHAp	5% B-nHAp	10% B-nHAp
1 : 1	$11.1 \pm 0.2^{a,A}$	$21.4 \pm 2.3^{a,B}$	$20.1 \pm 1.6^{a,B}$	$15.5 \pm 1.6^{a,AB}$
1 : 2	$106.5 \pm 10.9^{b,A}$	$78.2 \pm 3.2^{b,B}$	$65.4 \pm 5.8^{b,B}$	$50.2 \pm 8.1^{b,C}$
1 : 4	$134.5 \pm 18.1^{c,A}$	$87.4 \pm 4.6^{c,B}$	$104.6 \pm 13.1^{c,B}$	$101.9 \pm 10.1^{c,B}$
1 : 8	$156.9 \pm 22.1^{c,A}$	$84.9 \pm 6.2^{c,B}$	$109.9 \pm 16.5^{c,C}$	$117.1 \pm 16.2^{d,C}$
1 : 16	$94.1 \pm 8.3^{b,A}$	$91.3 \pm 5.2^{c,A}$	$115.1 \pm 17.7^{c,B}$	$128.6 \pm 10.7^{d,B}$
Control (DMEM)	100.0 ± 5.5^{b}	100.0 ± 5.5^{cd}	100.0 ± 5.5^{d}	100.0 ± 5.5^{c}

**Statistical difference between concentration rates of materials is shown as 'a-d', and statistical difference between nHAp and B-nHAp (1%, 5%, and 10%) is shown as 'A-C'; $p < 0.001$*

of boron did not have a significant effect on the morphological properties of nano-hydroxyapatite.

MTT TEST

Tables 1 and 2 show cell viability of nHAp and B-nHAp (1%, 5%, and 10%) on L929 mouse fibroblasts. The cell viability of nHAp and B-nHAp extracts (1%, 5%, and 10%) at the end of 24 hours showed statistically significant differences compared with the control group ($p < 0.001$). The extracts of nHAp in dilution ratios of 1 : 2 and 1 : 4 demonstrated more increased cell viability than the control group ($p < 0.001$). The extracts of 1%, 5%, and 10% B-nHAp all dilutions presented more decreased cell viability than the control group at the end of 24 hours (Figure 4). Statistically significant differences were observed in the cell viability of nHAp and B-nHAp extracts (1%, 5%, and 10%) at the end of 72 hours compared with the control group ($p < 0.001$). The extracts of nHAp in dilution ratios of 1 : 2, 1 : 4, and 1 : 8 showed higher cell viability than the control group ($p < 0.001$). The extracts of nHAp in 1 : 8 dilution ratio demonstrated the highest cell viability. The extracts of 1% B-nHAp in the whole dilution presented more decreased cell viability than the control group. However, the extracts of 5% and 10% B-nHAp in 1 : 4, 1 : 8, and 1 : 16 dilutions showed higher cell viability than the control group (Figure 5).

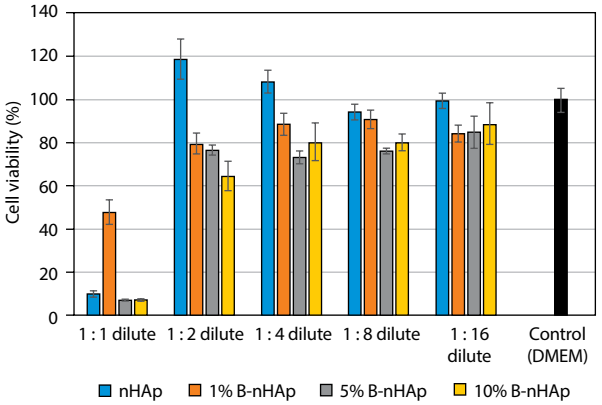

FIGURE 4. Cell viability percentages of the extracts of nHAp and B-nHAp (1%, 5%, and 10%) in different dilutions at the end of 24 hours

ANTIMICROBIAL ANALYSIS

Figure 6 displays the antibacterial effect of nHAp and B-nHAp (1%, 5%, and 10%) on *Streptococcus mutans*. Although nHAp particles showed the most antibacterial effect, the antibacterial effect decreased as the rate of nano-hydroxyapatite dilution increased ($p < 0.001$). B-nHAp at the rates of 1%, 5%, and 10% demonstrated less antibacterial effect than nHAp extracts ($p < 0.001$). The addition of boron to nano-hydroxyapatite did not increase antibacterial activity.

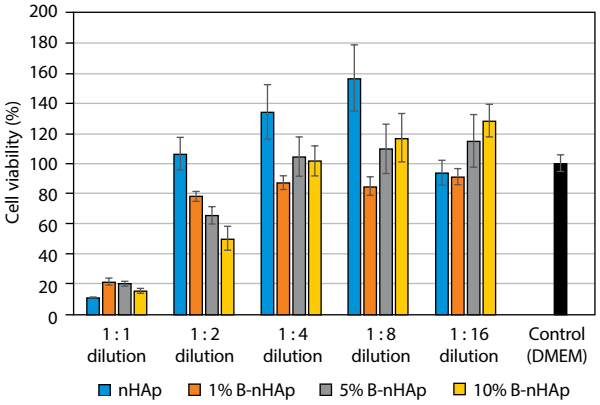

FIGURE 5. Cell viability percentages of the extracts of nHAp and B-nHAp (1%, 5%, and 10%) in different dilutions at the end of 72 hours

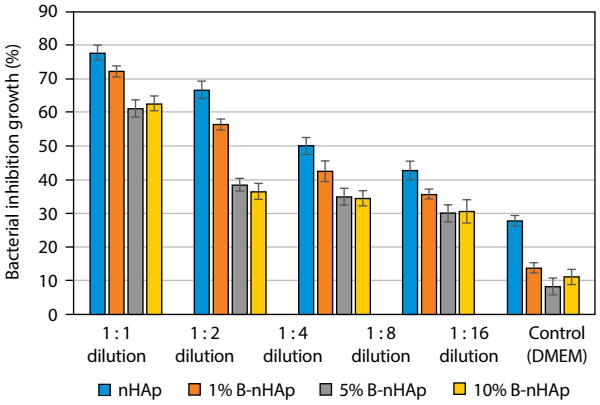

FIGURE 6. Relative bacterial growth inhibition (%) analysis of nHAp and B-nHAp (1%, 5%, and 10%) on *Streptococcus mutans* ATCC 25175

DISCUSSION

This study examined the cytotoxicity and antibacterial effect of B-nHAp synthesized at 1%, 5%, and 10% using nano-hydroxyapatite. The cytotoxicity of B-nHAp L929 on mouse fibroblast cells at DS was demonstrated in comparison with nHAp and B-nHAp. In addition, the antibacterial effect of nHAp and B-nHAp on *Streptococcus mutans* was examined using a modified microdilution method.

Nano-hydroxyapatite can form a protective layer by penetrating the enamel and dentin surfaces affected by caries attack [18, 20]. In early-stage caries, hard tissue loses mineral ions with acid attack from bacterial metabolism, but the collagen network remains unaffected. This attempt to re-mineralize organic scaffolding is carried out using nano-particles (nHAp), which act as a direct substitute for the final minerals or as a carrier for ions lost in caries attack [20].

Boron is generally released from biomaterials at low rates and in short periods [21]. In their study, Gizer *et al.* [22] reported that boron was released from the B-nHAp composite within the first hour, and that B-nHAp, nHAp composites, and/or boric acid changed the proliferation of bone cells and osteogenic differentiation depending on the dose and time. Hakki *et al.* [12] reported that a higher concentration of boron on MC3T3-E1 cells decreased the cell survival rate in a short time, but then this effect disappeared, and there was no toxic effect.

Saglam *et al.* [23] evaluated the toxicity of boric acid at different concentrations (6%, 3%, 1.5%, 0.75%, 0.375%, 0.1875%, and 0.09375%), and reported that boric acid below 0.75% was not toxic to gingival fibroblasts and periodontal ligament fibroblasts. Another study showed that 5 mg/ml – 2,000 mg/ml (0.0005% and 0.2%) concentrations were not toxic for these cells when the cytotoxicity of boric acid against adipose stem cells was evaluated using the MTS method [24]. The literature has reported that high boric acid concentrations cause a decrease in the pH of a medium, leading to harmful effects on cells that grow very well under neutral conditions [16].

In this study, a dose-dependent effect was observed on 1%, 5%, and 10% B-nHAp L929 mouse fibroblast cells. In addition, as the dilution rate of B-nHAp extracts increased (1 : 1, 1 : 2, 1 : 4, 1 : 8, and 1 : 16), the cell viability also increased. However, it showed less cell viability in the B-nHAp group than in the nHAp group after 24 and 72 hours.

Tooth decay is the localized destruction of dental hard tissue under the influence of acids produced by bacteria [25]. The primary pathogenic bacteria of dental caries are *Streptococcus mutans* [26]. Therefore, in the current study, the extracts were tested against *Streptococcus mutans*.

In the medical field, boric acid has been reported to have a bacteriostatic and bactericidal effect. Karaarslan *et al.* [27] reported that boric acid at concentrations of 0.5% and above could prevent the growth of *Aspergillus* and *Candida albicans*, and this effect was not observed at lower concentrations. Kanoriya *et al.* [28] reported that a 0.75% boric acid concentration could help significantly reduce periodontal pocket depth and gingival bleeding compared with a placebo group. Demirci *et al.* [11] reported that boron-containing composites showed a remarkable antibacterial effect against *Streptococcus mutans*, and increasing osteogenic and odontogenic differentiation capacity of hDPSCs. In our study, B-nHAp showed an antibacterial effect on *Streptococcus mutans* ATCC 25175. However, this antibacterial effect was found to be less than that of nHAp. Furthermore, the antibacterial effect on *Streptococcus mutans* decreased as the rate of nHAp and B-nHAp dilution increased.

An important limitation of this study is the use of only L929 mouse fibroblast cells. In this study, unlike the literature, the addition of boron to nano-hydroxyapatite did not significantly increase regenerative and

antibacterial properties of the material. Regenerative effects on pulp cells should be evaluated in future studies. Therefore, prospective studies are needed to prove the clinical suitability and applicability of B-nHAp in dentistry practice.

CONCLUSIONS

This study demonstrated that B-nHAp (1%, 5%, and 10%) decreased cell viability more than nHAp in L929 mouse fibroblasts. B-nHAp (1%, 5%, and 10%) showed less antibacterial effects on *Streptococcus mutans* than nHAp. As the rate of nHAp and B-nHAp dilutions increased, the regenerative effect on the cells increased, while the antibacterial effect decreased. The addition of boron to nano-hydroxyapatite does not make a significant contribution to increasing the regenerative and antibacterial properties of the materials.

DISCLOSURES

1. Institutional review board statement: Not applicable.
2. Assistance with the article: None.
3. Financial support and sponsorship: None.
4. Conflicts of interest: The authors declare no potential conflicts of interest concerning the research, authorship, and/or publication of this article.

References

1. Yang J, Yuan G, Chen Z. Pulp regeneration: current approaches and future challenges. Front Physiol 2016; 7: 58. DOI: 10.3389/fphys.2016.00058.
2. Miran S, Mitsiadis TA, Pagella P. Innovative dental stem cell-based research approaches: the future of dentistry. Stem Cells Int 2016; 2016: 7231038. DOI: 10.1155/2016/7231038.
3. Luukko K, Moe K, Sijaona A, Furmanek T, Kvinnsland IH, Midtbø M, Kettunen P. Secondary induction and the development of tooth nerve supply. Ann Anat 2008; 190: 178-187.
4. Zhao H, Feng J, Seidel K, Shi S, Klein O, Sharpe P, Chai Y. Secretion of shh by a neurovascular bundle niche supports mesenchymal stem cell homeostasis in the adult mouse incisor. Cell Stem Cell 2014; 14: 160-173.
5. Shi S, Gronthos S. Perivascular niche of postnatal mesenchymal stem cells in human bone marrow and dental pulp. J Bone Miner Res 2003; 18: 696-704.
6. Ratajczak J, Bronckaers A, Dillen Y, Gervois P, Vangansewinkel T, Driesen RB, et al. The neurovascular properties of dental stem cells and their importance in dental tissue engineering. Stem Cells Int 2016; 2016: 9762871. DOI: 10.1155/2016/9762871.
7. Zivkovic P, Petrovic V, Najman S, Gervois P, Vangansewinkel T, Driesen RB, et al. Stem cell-based dental tissue engineering. Sci World J 2010; 10: 901-916.
8. Chen Q, Roether J, Boccaccini A. Tissue engineering scaffolds from bioactive glass and composite materials. Top Tissue Eng 2008; 4: 1-27.
9. Gorustovich AA, López JMP, Guglielmotti MB, Cabrini RL. Biological performance of boron-modified bioactive glass particles implanted in rat tibia bone marrow. Biomed Mater 2006; 1: 100-105.
10. Taşlı PN, Doğan A, Demirci S, Şahin F. Boron enhances odontogenic and osteogenic differentiation of human tooth germ stem cells (hTGSCs) in vitro. Biol Trace Elem Res 2013; 153: 419-427.
11. Demirci S, Kaya MS, Doğan A, Kalay S, Kilicet NO, Yarat A, et al. Antibacterial and cytotoxic properties of boron-containing dental composite. Turk J Biol 2015; 39: 417-426.
12. Hakki SS, Bozkurt BS, Hakki E. Boron regulates mineralized tissue-associated proteins in osteoblasts (MC3T3-E1). J Trace Elem Med Biol 2010; 24: 243-250.
13. Ying X, Cheng S, Wang W, Lin Z, Chen Q, Zhang W, et al. Effect of boron on osteogenic differentiation of human bone marrow stromal cells. Biol Trace Elem Res 2011; 144: 306-315.
14. Movahedi Najafabadi BA, Abnosi MH. Boron induces early matrix mineralization via calcium deposition and elevation of alkaline phosphatase activity in differentiated rat bone marrow mesenchymal stem cells. Cell J 2016; 18: 62-73.
15. Demirer S, Kara M, I Erciyas K, Ozdemir H, Ozer H, Ay S. Effects of boric acid on experimental periodontitis and alveolar bone loss in rats. Arch Oral Biol 2012; 57: 60-65.
16. Pham TAV. In vitro characteristics of human periodontal ligament stem cells incubated with boric acid. J Oral Biosci 2020; 62: 155-161.
17. Bordea IR, Candrea S, Alexescu GT, Bran S, Băciuț M, Băciuț G, et al. Nano-hydroxyapatite use in dentistry: a systematic review. Drug Metab Rev 2020; 52: 319-332.
18. Souza BM, Comar LP, Vertuan M, Neto CF, Afonso Rabelo Buzalaf M, Magalhães AC. Effect of an experimental paste with hydroxyapatite nanoparticles and fluoride on dental demineralisation and remineralisation in situ. Caries Res 2015; 49: 499-507.
19. Tunçay EÖ, Demirtaş TT, Gümüşderelioğlu M. Microwave-induced production of boron-doped HAp (B-HAp) and B-HAp coated composite scaffolds. J Trace Elem Med Biol 2017; 40: 72-81.
20. Besinis A, van Noort R, Martin N. Remineralization potential of fully demineralized dentin infiltrated with silica and hydroxyapatite nanoparticles. Dent Mater 2014; 30: 249-262.
21. Gümüşderelioğlu M, Tunçay EÖ, Kaynak G, Demirtaş TT, Tığlı Aydın S, Hakkı SS. Encapsulated boron as an osteoinductive agent for bone scaffolds. J Trace Elem Med Biol 2015; 31: 120-128.
22. Gizer M, Köse S, Karaosmanoglu B, Taskiran EZ, Berkkan A, Timuçin M, et al. The effect of boron-containing nano-hydroxyapatite on bone cells. Biol Trace Elem Res 2020; 193: 364-376.
23. Saglam M, Arslan U, Buket Bozkurt S, Hakki SS. Boric acid irrigation as an adjunct to mechanical periodontal therapy in patients with chronic periodontitis: a randomized clinical trial. J Periodontol 2013; 84: 1297-1308.
24. Apdik H, Dogan A, Demirci S, Aydin S, Sahin F. Dose-dependent effect of boric acid on myogenic differentiation of human Adipose-derived stem cells (hADSCs). Biol Trace Elem Res 2015; 165: 123-130.
25. Strużycka I. The oral microbiome in dental caries. Polish J Microbiol 2014; 63: 127-135.
26. Høiby N, Ciofu O, Johansen HK, Song Z, Moser C, Jensen PØ, et al. The clinical impact of bacterial biofilms. Int J Oral Sci 2011; 3: 55-65.
27. Karaarslan A, Ozcan KM, Ozcan M. The efficacy of boric acid in otomycosis: a in vitro study. Mediterr Otol 2005; 1: 83-86.
28. Kanoriya D, Singhal S, Garg V, Pradeep AR, Garg S, Kumar A. Clinical efficacy of subgingivally-delivered 0.75% boric acid gel as an adjunct to mechanotherapy in chronic periodontitis: a randomized, controlled clinical trial. J Investig Clin Dent 2018; 9. DOI: 10.1111/jicd.12271.